J|A|C|S
ARTICLES
Published on Web 12/07/2005

Hydrophobicity, Shape, and π-Electron Contributions during Translesion DNA Synthesis

Xuemei Zhang,[‡] Irene Lee,*[,‡] Xiang Zhou,[§] and Anthony J. Berdis*[,†]

Contribution from the Departments of Pharmacology and Chemistry, Case Western Reserve University, 10900 Euclid Avenue, Cleveland, Ohio 44106, and Department of Chemistry, Cleveland State University, 2121 Euclid Avenue, Cleveland, Ohio 44115

Received July 13, 2005; E-mail: ixl13@case.edu; ajb15@cwru.edu

Abstract: Translesion DNA synthesis, the ability of a DNA polymerase to misinsert a nucleotide opposite a damaged DNA template, represents a common route toward mutagenesis and possibly disease development. To further define the mechanism of this promutagenic process, we synthesized and tested the enzymatic incorporation of two isosteric 5-substituted indolyl-2′deoxyriboside triphosphates opposite an abasic site. The catalytic efficiency for the incorporation of the 5-cyclohexene-indole derivative opposite an abasic site is 75-fold greater than that for the 5-cyclohexyl-indole derivative. The higher efficiency reflects a substantial increase in the k_{pol} value (compare 25 versus 0.5 s^{-1}, respectively) as opposed to an influence on ground-state binding of either non-natural nucleotide. The faster k_{pol} value for the 5-cyclohexene-indole derivative indicates that π-electron density enhances the rate of the enzymatic conformational change step required for insertion opposite the abasic site. However, the kinetic dissociation constants for the non-natural nucleotides are identical and indicate that π-electron density does not directly influence ground-state binding opposite the DNA lesion. Surprisingly, each non-natural nucleotide can be incorporated opposite natural templating bases, albeit with a greatly reduced catalytic efficiency. In this instance, the lower catalytic efficiency is caused by a substantial decrease in the k_{pol} value rather than perturbations in ground-state binding. Collectively, these data indicate that the rate of the conformational change during translesion DNA synthesis depends on π-electron density, while the enhancement in ground-state binding appears related to the size and shape of the non-natural nucleotide.

Introduction

Translesion DNA synthesis represents the ability of a DNA polymerase to insert opposite and extend beyond a DNA lesion. This process is promutagenic since the polymerase typically misinserts an incorrect nucleotide opposite the DNA lesion.[1] One commonly formed DNA lesion is an abasic site that can be produced nonenzymatically[2] or through the action of DNA repair enzymes.[3] This lesion is highly mutagenic since it is devoid of hydrogen-bonding potential. Despite the nontemplating nature of an abasic site, most DNA polymerases preferentially incorporate dATP (**1**) opposite this lesion.[4] Several mechanisms including steric constraints[5] and desolvation[6] have been proposed to account for this kinetic phenomenon. An alternative mechanism to explain the preferential incorporation of dATP is that the efficiency of insertion is influenced by the base-stacking capabilities of the incoming nucleotide.[7,8] The validity of this hypothesis has been strengthened by the favorable enzymatic incorporation of non-natural nucleotides such as 5-NITP (**2**) and 5-PhITP (**3**) opposite this DNA lesion.[9,10] Both analogues have substituent groups rich in π-electron density, a feature that provides greater base-stacking capabilities compared to natural dNTPs. Remarkably, the catalytic efficiency for the incorporation of **2** and **3** opposite an abasic site is ~1,000-fold greater than that measured for dATP incorporation.[9,10] Furthermore, replacement of the nitro or phenyl moiety with functional groups such as $-H$, $-F$, or $-NH_2$ that are lacking π-electron density reduces the efficiency of insertion by 3 orders of magnitude.[11] These data collectively indicate that the presence of π-electron density significantly enhances nucleotide incorporation opposite damaged DNA.

Although 5-NITP and 5-PhITP are preferentially inserted opposite an abasic site, these analogues are also incorporated

[†] Department of Pharmacology, Case Western Reserve University.
[‡] Department of Chemistry, Case Western Reserve University.
[§] Cleveland State University.

(1) (a) Wagner, J.; Etienne, H.; Janel-Bintz, R.; Fuchs, R. P. *DNA Repair (Amst)* **2002**, *1*, 159−167. (b) Pages, V.; Fuchs, R. P. *Oncogene* **2002**, *21*, 8957−8966.
(2) Lindahl, T. *Nature* **1993**, *362*, 709−715.
(3) Boiteux, S.; Guillet, M. *DNA Repair (Amst)* **2004**, *3*, 1−12.
(4) (a) Schaaper, R. M.; Kunkel, T. A.; Loeb, L. A. *Proc. Natl. Acad. Sci. U.S.A.* **1983**, *80*, 487−491. (b) Boiteux, S.; Laval, J. *Biochemistry* **1982**, *21*, 6746−6751. (c) Efrati, E.; Tocco, G.; Eritja, R.; Wilson, S. H.; Goodman, M. F. *J. Biol. Chem.* **1997**, *272*, 2559−2569. (d) Mozzherin, D. J.; Shibutani, S.; Tan, C.-K.; Downey, K. M.; Fisher, P. A. *Proc. Natl. Acad. Sci. U.S.A.* **1997**, *94*, 6126−6131.
(5) (a) Kool, E. T. *Annu. Rev. Biophys. Biomol. Struct.* **2001**, *30*, 1−22. (b) Matray, T. J.; Kool, E. T. *Nature* **1999**, *399*, 704−709.
(6) (a) Vesnaver, G.; Change, C. N.; Eisenberg, M.; Grollman, A. P.; Breslauer, K. J. *Proc. Natl. Acad. Sci. U.S.A.* **1989**, *86*, 3614−3618. (b) Goodman, M. F.; Ceighton, S.; Bloom, L. B.; Petruska, J. *Crit. Rev. Biochem. Mol. Biol.* **1993**, *28*, 83−126.
(7) Cuniasse, P.; Fazakerley, G. V.; Guschlbauer, W.; Kaplan, B. E.; Sowers, L. C. *J. Mol. Biol.* **1987**, *213*, 303−314.
(8) Berdis, A. J. *Biochemistry* **2001**, *40*, 7180−7191.
(9) Reineks, E. Z.; Berdis, A. J. *Biochemistry* **2004**, *43*, 393−404.
(10) Zhang, X.; Lee, I.; Berdis, A. J. *Biochemistry*, **2005**, *44*, 13101−13110.
(11) Zhang, X.; Lee, I.; Berdis, A. J. *Org. Biomol. Chem.* **2004**, *2*, 1703−1711.

opposite all templating nucleobases with reduced efficiencies.[9,10] Both nucleotides bind with high affinity (K_D values of ~20 μM) regardless of templating position. This feature suggests that π-electron density contribute significantly toward the ground-state binding of a nucleotide. In fact, the lack of selectivity for incorporation coupled with the low K_D values were argued to reflect the presence of a "nonspecific" dNTP binding site that utilized $\pi-\pi$ stacking interactions between the aromatic rings of the incoming dNTP and amino acids.[9] To further define this hypothetical mechanism, we characterized the incorporation of two isosteric analogues of 5-PhITP (**3**) that possess different π-electron densities. The nucleotide containing π-electron density is incorporated opposite an abasic site 50-fold faster than the isosteric analogue devoid of this feature. However, the kinetic dissociation constants for the non-natural nucleotides are identical and indicate that π-electron density does not directly influence ground-state binding opposite the DNA lesion. These data are interpreted with respect to a model in which π-electron density enhances the rate of the enzymatic conformational change step required for insertion opposite the abasic site while binding affinity is driven by the hydrophobicity and size of the nucleotide substrate.

Experimental Section

General. Tributylammonium pyrophosphate was purchased from Sigma. Other reagents such as sodium hydride, sodium methoxide, and phosphoryl oxychloride were purchased from ACROS. Trimethyl phosphate and tributylamine were dried over 4 Å molecular sieves. DMF was distilled over ninhydrin, stored in 4 Å molecular sieves. All NMR spectra were recorded in a Gemini-300 FT NMR spectrometer. Proton chemical shifts are reported in ppm downfield from tetramethylsilane (TMS). Coupling constants (J) are reported in hertz (Hz). ^{31}P NMR spectra were obtained in D_2O in the presence of 50 mM Tris (PH 7.5) and 2 mM EDTA. Phosphoric acid (85%) was used as external standard. UV absorptions were measured using Beckman DU-70 spectrometer. Both low- and high-resolution positive fast atom bombardment mass spectra [FAB-MS (+)] were obtained with a Kratos MS-25RFA spectrometer at Case Western Reserve University. LC-MS was performed at Cleveland State University. High-resolution electrospay mass spectrometry [HiRes ESI-MS] was performed on an IonSpec HiRes ESI-FTICRMS at the University of Cincinnati.

Synthesis of 5-(1-Hydroxylcyclohexyl)indole (7a). 5-Bromoindole (**6**) (8 g, 40 mmol) in 80 mL of anhydrous THF was added to a solution of KH (5.89 g, 41 mmol) in 80 mL of anhydrous THF at 0 °C. The reaction mixture was stirred for 15 min and then cooled to −78 °C. *tert*-Butyllithium (60 mL, 90 mmol) prechilled to −78 °C was added via cannula. After 30 min, cyclohexanone (8 g, 8.26 mL, 80 mmol) in THF (40 mL) was introduced. The reaction mixture was slowly warmed to room temperature (about 2 h) and then poured into an ice-cold solution of 1 M H_3PO_4 (150 mL). The aqueous phase was extracted with EtOAc (3 × 100 mL). The organic phases were combined and washed with $NaHCO_3$ solution, and then saturated NaCl. The resulting organic layer was dried over $MgSO_4$, filtered, and concentrated to dryness. The resulting crystal was washed with hexane to yield 6 g of the product. H NMR ($CDCl_3$) δ 1.60−1.90 (10H, m, CH_2), 6.5 (1H, s, 3-H), 7.1 (1H, s, Ar), 7.4 (2H, s, Ar), 7.8 (1H, s, Ar), 8.15 (1H, br s, NH). HiRes FAB-MS (+): Calculated mass spectra (formula: $C_{14}H_{17}NO$ for M), 215.13101; Experimental mass spectra, 215.13159. C NMR ($CDCl_3$) δ 22.55, 25.74, 39.35, 73.43, 102.90, 110.79, 116.42, 119.53, 124.61, 127.69, 134.77, 141.08.

Synthesis of 5-Cyclohexylindole (7c). To anhydrous THF in an ice-bath was added 1.14 g (30 mmol) of $LiAlH_4$ and then 3.6 g (28 mmol) of $AlCl_3$. After 5 min, 3 g of 5-(1-hydroxylcyclohexyl)indole (**7a**) (14 mmol) was added, and the reaction mixture was refluxed for 2 h before cooling in an ice bath and quenched with H_2O. A solution of saturated $NaHCO_3$ was added to neutralize the reaction, from which the organic and the aqueous phases were separated. The aqueous phase, which contained inorganic solid, was extracted with EtOAc 4 times. The organic phases were pooled, washed with saturated NaCl, dried over $MgSO_4$, filtered, and then evaporated to dryness. The residue was purified by silica flash chromatography using hexane as the eluent to yield 1.4 g of product. H NMR ($CDCl_3$) δ 1.5 (6H, m, CH_2), 1.8 (4H, m, CH_2), 2.6 (1H, m, CH), 6.5 (1H, s, 3-H) 7.1 (1H, d, J = 9.0 Hz, Ar), 7.2 (1H, s, Ar), 7.35 (1H, d, J = 9.0 Hz, Ar), 7.50 (1H, s, Ar), 8.15 (1H, br s, NH). HiRes FAB-MS (+): Calculated mass spectra (formula $C_{14}H_{17}NO$ for M), 199.13610; Experimental mass spectra, 199.13610. C NMR ($CDCl_3$) δ 26.36, 27.20, 35.23, 44.74, 102.46, 110.68, 118.02, 121.79, 124.22.

Synthesis of 1-(3,5-Di-*O*-*p*-toluoyl-2-deoxy-*β*-D-*erythro*pentafuranosyl)-5-(1-hydroxyl)-cyclohexylindole (9a). To a solution of 5-(1-hydroxylcyclohexyl)indole (**7a**) (0.8 g, 4 mmol) in dry acetonitrile (100 mL) was added 0.35 g of NaH (9 mmol). The reaction was stirred at room temperature for 90 min before the addition of 2.4 g of 1-chloro-2-deoxy-3,5-di-*O*-*p*-toluoyl-α-D-*erythro*pentofuranose (**8**) (6 mmol). The resulting mixture was further stirred at room temperature for 16 h, filtered, and then evaporated to dryness. The crude product was purified by silica flash column chromatography using toluene as the eluent to yield 1.5 g of colorless oil. H NMR ($CDCl_3$) δ 1.60−1.90 (10H, m, CH_2), 2.43 (3H, s, CH_3), 2.45 (3H, s, CH_3), 2.63 (1H, m, 2′-H), 2.87 (1H, m, 2′-H), 4.57 (1H, m, 4′-H), 4.63 (2H, m, 5′-H), 5.72 (1H, m, 3′-H), 6.44 (1H, t, J = 7.5 Hz, 1′-H), 6.55 (1H, d, J = 3 Hz, 3-H), 7.20−7.32 (6H, m, Ar), 7.50 (1H, d, J = 9.0, Ar), 7.75 (1H, s, Ar), 7.95 (4H, m, Ar). HiRes FAB-MS (+): Calculated mass spectra (formula: $C_{35}H_{37}NO_6$ for M), 567.26209; Experimental mass spectra, 567.26003.

Synthesis of 1-(3,5-Di-*O*-*p*-toluoyl-2-deoxy-*β*-D-*erythro*pentafuranosyl)-5-cyclohexylindole (9c). This compound was prepared and purified by the method described for 1-(3,5-di-*O*-*p*-toluoyl-2-deoxy-*β*-D-*erythro*pentafuranosyl)-5-(1-hydroxyl)cyclohexylindole (**9a**) using 5-cyclohexylindole (**7c**) (0.8 g, 4 mmol) as the starting material. The product was a light yellow oil, and the yield was 1.5 g. H NMR ($CDCl_3$) δ 1.45 (6H, m, CH_2), 1.90(4H, m, CH_2), 2.43 (3H, s, CH_3), 2.45 (3H, s, CH_3), 2.55 (1H, m, CH), 2.65 (1H, m, 2′-H), 2.87 (1H, m, 2′-H), 4.57 (1H, m, 4′-H), 4.63 (2H, m, 5′-H), 5.72 (1H, m, 3′-H), 6.44 (1H, dd, J = 7.5 Hz, 6 Hz, 1′-H), 6.48 (1H, d, J = 3 Hz, 3-H), 7.02 (1H, d, J = 9.0, Ar), 7.20−7.45 (7H, m, Ar) 7.95 (4H, m, Ar). HiRes ESI-MS (+): Calculated mass spectra (formula $C_{35}H_{38}NO_5$ for M + H), 552.2750; Experimental mass spectra, 552.2758.

Synthesis of 1-(2-Deoxy-α,*β*-D-*erythro*pentafuranosyl)-5-cyclohexenylindole (10b). To 30 mg of 1-(3,5-di-*O*-*p*-toluoyl-2-deoxy-*β*-D-*erythro*pentafuranosyl)-5-(1-hydroxyl)cyclohexylindole **9a** (0.05 mmol) in 10 mL of THF was added 15 mg of $AlCl_3$ (0.1 mmol). The reaction mixture was stirred at room temperature until completion as determined by TLC (approximately 45 min). The resulting reaction intermediate **9b** was used in the next step without further purification. To **9b** was then added a solution of sodium methoxide in methanol until the pH of the reaction mixture reached >12. The reaction stirred at room temperature for 16 h before being evaporated to dryness. The resulting residue was purified by silica flash chromatography using dichloromethane−methanol, 95:5 as eluent. A 1:1 mixture of *a*- and *β*-anomers were obtained. The product mixture was a light purple oil and the yield was 8 mg. H NMR (DMSO) δ 1.60 (2H, m, CH_2), 1.75 (2H, m, CH_2), 2.20 (3H, m, CH_2 and 2′-H), 2.50 (3H, m, CH_2 and 2′-H), 3.50 (2H, m, 5′-H), 3.80, 3.95 (1H, m, 4′-H), 4.29 (1H, m, 3′-H), 4.75, 4.85 (1H, m, 5′-OH), 5.28, 5.40 (1H, m, 3′-OH), 6.06 (1H, m, CH), 6.33 (1H, t, J = 7.0 Hz, 1′-H), 6.43 (1H, s, 3-H), 7.2 (1H, m, Ar), 7.5 (2H, m, Ar), 7.65 (1H, s, Ar). UV (MeOH) λ_{max} (nm): 240, 266 (ϵ = 8540 M^{-1} cm^{-1}), 292 (sh). HiRes ESI-MS (+): Calculated mass spectra (formula $C_{19}H_{24}NO_3$ for M + H), 314.1756; Experimental mass spectra, 314.1749.

Synthesis of 1-(2-Deoxy-β-D-*erythro*pentafuranosyl)-5-cyclohexylindole (10c). To 1.5 g of 1-(3,5-di-*O*-*p*-toluoyl-2-deoxy-β-D-*erythro*-pentafuranosyl)-5-cyclohexylindole **9c** (2.7 mmol) in methanol (50 mL) and ether (15 mL) was added solid sodium methoxide until the pH of the solution reached 12. The mixture was stirred at room temperature for 16 h and then evaporated to dryness. The resulting residue was treated with 3 mL of MeOH, from which the methanolic solution was filtered, and then evaporated to dryness. The crude product was further purified by silica flash chromatography, dichloromethane−methanol 95:5 as eluent, to yield 570 mg of a colorless crystal as the final product. H NMR (DMSO) δ 1.40 (6H, m, CH_2), 1.80 (4H, m, CH_2), 2.16 (1H, m, 2′-H), 2.45 (1H, m, 2′-H), 2.50 (1H, m, CH), 3.50 (2H, m, 5′-H), 3.80 (1H, m, 4′-H), 4.31 (1H, m, 3′-H), 4.85 (1H, m, 5′-OH), 5.28 (1H, m, 3′-OH), 6.30 (1H, t, $J = 7.5$ Hz, 1′-H), 6.45 (1H, d, $J = 3.4$ Hz, 3-H), 7.01 (1H, d, $J = 9.0$ Hz, Ar), 7.35 (1 H, s, Ar), 7.45 (1H, d, $J = 9.0$, Ar), 7.50 (1H, d, $J = 3$ Hz, Ar). UV (MeOH) λ_{max} (nm) 266 ($\epsilon = 6843$ M^{-1} cm^{-1}). Upon irradiation at 6.30 ppm for the anomeric hydrogen, the NOE observed at 3.80 (H-4′, 0.52%) along with 2.16 (H-2′α, 3.1%), 7.45 (H-2, 3.21%), 7.50 (H-7, 1.10%). HiRes ESI-MS (+): Calculated mass spectra (formula $C_{19}H_{26}NO_3$ for M + H), 316.1913; Experimental mass spectra, 316.1899.

Preparation of Indole Derivative Triphosphates. Phosphoryl oxychloride (16 μL, 3 mol equiv, 0.18 mmol) was added dropwise to a stirred and cooled (0 °C) solution of 2′-deoxynucleoside (20 mg, 0.06 mmol) and triethylamine (34 mg, 5 equiv, 0.33 mmol) in trimethyl phosphate (0.37 mL). The reaction was monitored on TLC, and after 1.5 h, about 50% conversion had occurred. The reaction mixture was then treated with a 0.5 M solution of tributylammonium pyrophosphate (400 mg, 0.75 mmol) in DMF and tributylamine (0.18 mL, 0.75 mmol). Upon stirring at room temperature for 20 min, the reaction was neutralized with 1.0 M TEAB (15 mL) and then stirred at room temperature for an additional 2 h. The final reaction mixture was evaporated under reduced pressure at 32 °C to about 2 mL. The resulting residue was purified by preparative reversed phase HPLC (300 pore size C-18 column from Vydac, 22 mm × 250 mm) using a linear gradient of 50% to 80% B within 14 min at a flow rate of 17.00 mL/min (mobile phase buffer A, 0.1 M TEAB; buffer B, 50% ACN in 0.1 M TEAB). Both α and β isomers of the triphosphates were separately collected and characterized by mass spectrum and NMR spectroscopy. The resulting products were evaporated to 1 mL under reduced pressure at 32 °C, redissolved in 5 mL of methanol, and then evaporated to dryness. This process was repeated 3 times. The final product was dissolved and stored in 10 mM Tris HCl, pH 7.5. The concentration of the triphosphate was determined by UV absorbance of the nucleoside at 266 nm. The extinction coefficients for 5-CEITP (**4**) and 5-CHITP (**5**) at 266 nm are 8540 M^{-1} cm^{-1} and 6843 M^{-1} cm^{-1}, respectively.

Synthesis of 1-(2-Deoxy-D-*erythro*pentafuranosyl)-5-cyclohexenylindole Triphosphate (4). This compound was synthesized and purified according to the general method described above, using 1-(2-deoxy-D-*erythro*pentafuranosyl)-5-cyclohexenylindole as the starting material (**10b**). A mixture of α- and β-isomers was obtained. Characterization of the α-isomer is provided as Supporting Information. The β-isomer of the triphosphate was eluted at 70.9% B (9.8 min retention time) in preparative reversed phase HPLC. H NMR (D_2O) δ 1.55 (2H, m, CH_2), 1.65 (2H, m, CH_2), 2.09 (2H, m, CH_2), 2.20 (1H, m, 2′-H), 2.32 (2H, m, CH_2), 2.65 (1H, m, 2′-H), 3.95 (2H, m, 5′-H), 4.05 (1H, m, 4′-H), 6.10 (1H, m, CH), 6.40 (1H, m, 1′-H), 6.50 (1H, d, $J = 3$ Hz, 3-H), 7.30 (1H, t, $J = 7.5$ Hz, Ar), 7.40 (2H, m, Ar), 7.55 (1H, d, $J = 7.5$, Ar). HiRes ESI-MS (−): Calculated mass spectra (formula: $C_{19}H_{25}NO_{12}P_3$ for M − H), 552.0590; Experimental mass spectra, 552.0704.

Synthesis of 1-(2-Deoxy-D-*erythro*pentafuranosyl)-5-cyclohexylindole Triphosphate (5). This compound was synthesized and purified according to the general method described above, using 1-(2-deoxy-β-D-*erythro*pentafuranosyl)-5-cyclohexylindole (**10c**) as the starting material. A mixture of α- and β-isomers was obtained. The β-isomer of the triphosphate was eluted at 74.2% B (11.3 min retention time) in preparative reversed phase HPLC. Yield: 4%. H NMR (D_2O) δ 1.25 (6H, m, CH_2), 1.70 (4H, m, CH_2), 2.22 (1H, m, 2′-H), 2.45 (1H, m, CH), 2.60 (1H, m, 2′-H), 3.95 (2H, m, 5′-H), 4.05 (1H, m, 4′-H), 4.58 (1H, m, 3′-H), 6.35 (1H, dd, $J = 8.0$ Hz, 6.0 Hz, 1′-H), 6.40 (1H, d, $J = 3.4$ Hz, 3-H), 7.10 (1H, d, $J = 8.3$ Hz, Ar) 7.4 (3H, m, Ar). ^{31}P NMR (D_2O/Tris) δ γ-P, −7.18; α-P, −10.55; β-P, −21.64. HiRes ESI-MS (−): Calculated mass spectra (formula: $C_{19}H_{25}NO_{12}P_3$ for M − H), 554.0746; Experimental mass spectra, 554.0842.

Enzymatic Characterization of the Incorporation of (4) and (5) Opposite an Abasic Site or Templating DNA. Enzyme Assays. The assay buffer used in all kinetic studies consisted of 25 mM Tris-OAc (pH 7.5), 150 mM KOAc, and 10 mM 2-mercaptoethanol. All assays were performed at 25 °C. Polymerization reactions were monitored by analysis of the products on 20% sequencing gels as previously described (24). Gel images were obtained with a Packard PhosphorImager using the OptiQuant software supplied by the manufacturer. Product formation was quantified by measuring the ratio of ^{32}P-labeled extended and nonextended primer. The ratios of product formation are corrected for substrate in the absence of polymerase (zero point). Corrected ratios are then multiplied by the concentration of primer/template used in each assay to yield total product. All concentrations are listed as final solution concentrations.

The kinetic parameters, k_{pol}, K_D, and k_{pol}/K_D, for nucleotide **5** were obtained by monitoring the rate of product formation using a fixed amount of gp43 (50 nM) and DNA substrate (1,000 nM) at varying concentrations of nucleotide triphosphate (0.01−1 mM). Aliquots of the reaction were quenched into 0.5 M EDTA, pH 7.4 at times ranging from 5 to 600 s. Samples were diluted 1:1 with sequencing gel load buffer, and products were analyzed for product formation by denaturing gel electrophoresis. In all cases, steady-state rates were obtained from the linear portion of the time course. Data obtained for steady-state rates in DNA polymerization measured under pseudo-first-order reaction conditions were fit to eq 1

$$y = mt + b \tag{1}$$

where m is the slope of the line, b is the y-intercept, and t is time. The slope of the line is equivalent to the rate of the reaction, v, and has units of nM/s. Data for the dependency of v as a function of dXTP concentration were fit to the Michaelis−Menten equation

$$v = V_{max}[\text{dXTP}]/K_D + [\text{dXTP}] \tag{2}$$

where v is the rate of the reaction, V_{max} is the maximal velocity, K_D is the Michaelis constant for dXTP, and dXTP is the concentration of non-natural nucleotide substrate. k_{cat} is defined as V_{max}/[gp43].

Pre-Steady-State Nucleotide Incorporation Assays. A rapid quench instrument (KinTek Corporation, Clarence, PA) was used to monitor the time courses for the incorporation of nucleotide 4 opposite an abasic. Experiments were performed using single turnover reaction conditions. 1000 nM gp43 exo^- was incubated with 250 nM DNA in assay buffer containing EDTA (100 μM) and mixed with variable concentrations of nucleotide analogue (5−500 μM) and 10 mM MgAcetate. The reactions were quenched with 500 mM EDTA at variable times (0.005−10 s) and analyzed as described above. Data obtained for single turnover DNA polymerization assays were fit to eq 3

$$y = Ae^{-kt} + C \tag{3}$$

where A is the burst amplitude, k is the observed rate constant for initial product formation, t is time, and C is a defined constant.

Results and Discussions

Abasic sites are commonly formed DNA lesions that are potentially mutagenic due to the lack of hydrogen-bonding

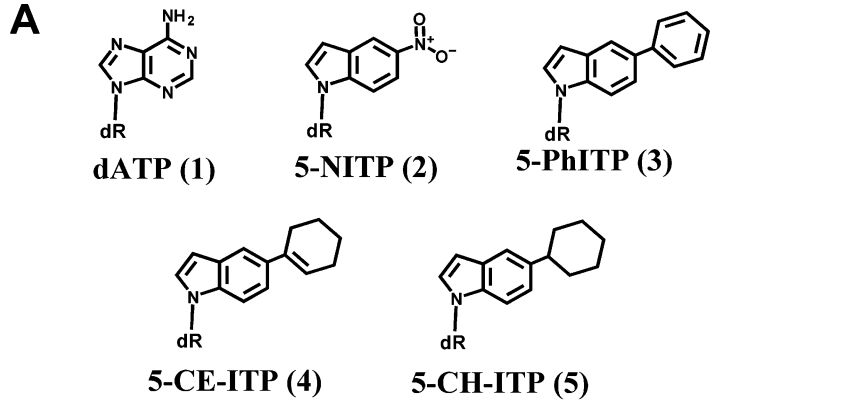

Figure 1. (A) Structures of 2′-deoxynucleoside triphosphates used or referred to in this study. For convenience, dR is used to represent the deoxyribose triphosphate portion of the nucleotides. (B) Defined DNA substrates used for kinetic analysis. "X" in the template strand denotes any of the four natural nucleobase or the presence of a tetrahydrofuran moiety designed to functionally mimic an abasic site.

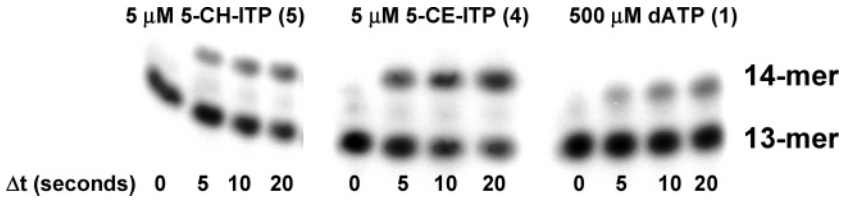

Figure 2. Comparison of the efficiency of insertion for non-natural and natural nucleoside triphosphates opposite an abasic site.

potential. Although most DNA polymerases involved in chromosomal replication preferentially incorporate dATP (**1**) opposite this lesion, the underlying mechanism accounting for its preferential remains undefined. We proposed based upon kinetic studies measuring the incorporation of non-natural nucleotides that that the presence of π-electron density significantly enhances nucleotide incorporation opposite this form of DNA damage. In this mechanism, initial ground-state binding is enhanced through $\pi-\pi$ stacking interactions between the aromatic amino acids lining the polymerase's active site with and the π-electrons present on the non-natural nucleotide. Furthermore, the rate of catalysis is enhanced through stacking interactions of the non-natural nucleotide inside the DNA helix. To further evaluate this proposed mechanism, we characterized the incorporation of two isosteric nucleotide analogues that possess differences in π-electron densities. One analogue, the 5-cyclohexene derivative **4** contains limited π-electron density by virtue of the presence of a double bond, while the 5-cyclohexylindolyl derivatives **5** is devoid of π-electron density (Figure 1A). Each analogue was synthesized as shown in Scheme 1 using established protocols.[11,12] Briefly, hydroxylcyclohexylindole **7a** was obtained using the protocol developed by Moyer et al.[12] Reduction with lithium aluminum hydride in the presence of a Lewis acid offered cyclohexylindole **7c**. The protected hydroxycyclohexylindole nucleoside **9a** and cyclohexylindole nucleoside **9c** were generated as a β anomeric isomer using the protocol of Girgis et al.[12] Dehydration of hydroxycyclohexylindole nucleoside **9a**, followed by deprotection of the hydroxyl groups in the sugar ring under basic condition, offered the cyclohexenylindole nucleoside (**10b**) as a mixture of α and β anomers. Deprotection of **9c** in basic condition yielded only the β anomeric isomer of **10c**. Both cyclohexenylindole and cyclohexylindole triphosphates (**4** and **5**) were prepared with a modified procedure from Zhang et al.,[11] using triethylamine as a base. For the synthesis of both triphosphates, α and β isomers were formed and well resolved by the reversed phase C-18 column. Only β isomers were used for the kinetic study.

The ability of these nucleotide analogues to be inserted opposite an abasic site was quantified by measuring the rate of primer elongation using the DNA substrate depicted in Figure 1B. The studies here continue to use the exonuclease-deficient form of the bacteriophage T4 DNA polymerase, gp43 exo$^-$, as the model enzyme. Initial experiments were performed under pseudo-first-order reaction conditions in which 5 μM nucleotide **4** or nucleotide **5** was added to a preincubated solution of 50 nM gp43 exo$^-$ and 1 μM 13/20SP-mer in the presence of 10 mM Mg^{2+}. As a positive control, experiments were also performed under identical conditions except that 500 μM dATP (**1**) was used as a natural nucleotide. Representative data provided in Figure 2 indicate that both non-natural nucleotides **4** and **5** are incorporated more effectively compared to natural purine substrate **1**. However, it is also clear that the cyclohexene derivative **4** is incorporated faster opposite the lesion compared

(12) (a) Moyer, M. P.; Shiurba, J. F.; Rapoport, H. *J. Org. Chem.* **1986**, *51*, 5106−5110. (b) Girgis, N. S.; Cottam, H. B.; Robins, R. K. *J. Heterocycl. Chem.* **1988**, *25*, 361. (c) Loakes, D.; Brown, D. M.; Linde, S.; Hill, F. *Nucleic Acids Res.* **1995**, *23*, 2361−2366.

Scheme 1 [a]

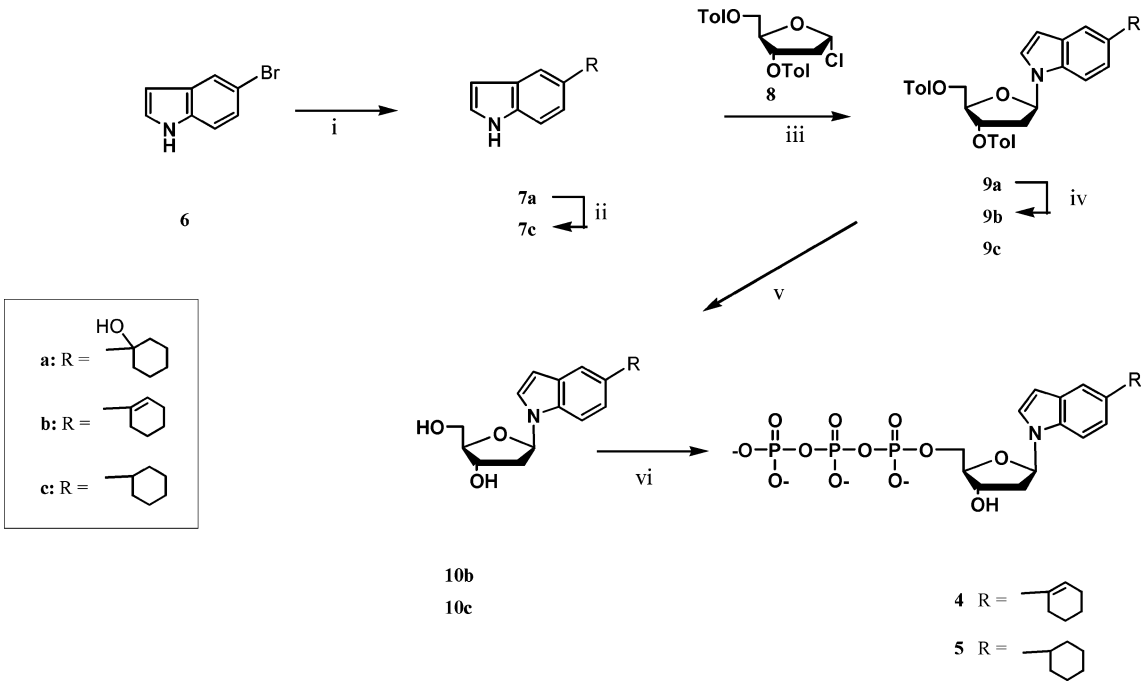

[a] Reagents and conditions: (i) (1) KH, THF; (2) *t*-BuLi, THF; (3) Cyclohexanone; (4) 1 M H_3PO_4. (ii) $LiAlH_4$, $AlCl_3$, THF. (iii) NaH, CH_3CN. (iv) $AlCl_3$, THF. (v) NaOMe/Methanol. (vi) (1) Trimethyl phosphate, 0 °C, $POCl_3$, Et_3N; (2) Bu_3N, $(Bu_3NH)_2H_2P_2O_7$ in DMF, 10 min; (3) 1 M $Et_3N{\cdot}H_2CO_3$.

to the cyclohexyl derivative **5**. Although these data suggest that π-electron density is important for effective insertion opposite the lesion, they cannot be used to unambiguously determine if the enhancement in insertion reflects an increase in binding affinity or through an increase in the rate of the conformational change step required for phosphoryl transfer.

To evaluate this question, K_D and k_{pol} values were measured for both non-natural nucleotides during incorporation opposite the lesion. Since the rates of nucleotide **4** incorporation were extremely fast (>100 nM/sec), a rapid quench instrument[13] was used to accurately monitor the kinetics of nucleotide incorporation. Experiments were performed using single turnover reaction conditions in which 1 μM gp43 exo$^-$ was incubated with 350 nM 13/20SP-mer in assay buffer containing EDTA (100 μM) and mixed with variable concentrations of nucleotide analogue (5−75 μM) and 10 mM Mg^{2+}. Figure 3A shows representative data for the concentration dependency of nucleotide **4** on the rate constant in primer elongation. All time courses were fit to the equation for a single-exponential process to define k_{obs}, the rate constant in product formation. The plot of k_{obs} versus the concentration of nucleotide **4** is hyperbolic (Figure 3B), and a fit of the data to the Michaelis−Menten equation[14] yields a k_{pol} value of 25.3 ± 1.9 s^{-1} and a K_D value of 5.1 ± 1.7 μM. Similar analyses were performed monitoring the incorporation of nucleotide **5** opposite the abasic site. Data for the rate of nucleotide incorporation as a function of nucleotide concentration were fit to the Michaelis−Menten equation to yield a k_{pol} value of 0.46 ± 0.03 s^{-1} and a K_D value of 6.2 ± 1.3 μM. Values are summarized in Table 1.

The fast k_{pol} value of ~25 s^{-1} measured for the incorporation of nucleotide **4** opposite an abasic site rivals that of 120 s^{-1} and 50 s^{-1} measured for the incorporation of the non-natural nucleotides **2**[9] and **3**,[10] respectively. In contrast, there is a 50-fold reduction in the k_{pol} value of compound **5** that clearly reflects the effects of removing π-electron density during translesion DNA synthesis. The difference in k_{pol} values

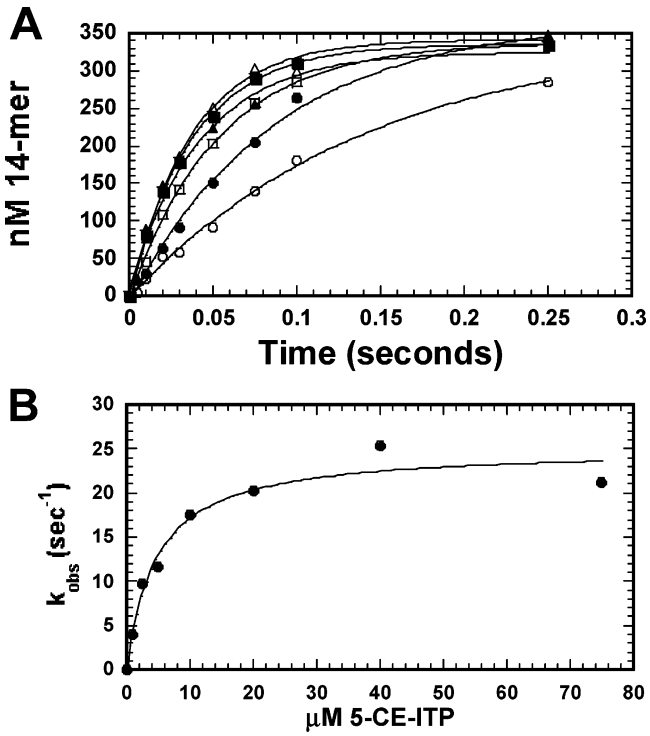

Figure 3. (A) Dependency of 5-CE-ITP concentration on the apparent burst rate constant as measured under single turnover conditions. 5-CE-ITP concentrations were 1 μM (○), 2.5 μM (●), 5 μM (□), 10 μM (▲), 20 μM (■), 40 μM (+), and 70 μM (△). The solid lines represent the fit of the data to a single exponential. (B) The observed rate constants for 5-CE-ITP insertion (●) were plotted against 5-CE-ITP concentration and fit to the Michaelis−Menten equation to determine values corresponding to K_d and k_{pol}.

(13) Johnson, K. A. *Methods Enzymol.* **1995**, *249*, 38−61.
(14) Ferscht, A. *Enzyme Structure and Mechanism*; W. H. Freeman and Company: New York; pp 98−101.

Table 1. Summary of Kinetic Rate and Dissociation Constants for the Insertion of 5-Cyclohexeneindolyl-2′-deoxyriboside Triphosphate and 5-cyclohexylindolyl-2′-deoxyriboside Triphosphate Opposite Templating and Nontemplating Nucleobases

dXTP	template	k_{pol} (s^{-1})	K_D (μM)	k_{pol}/K_D ($M^{-1}\,s^{-1}$)
5-CE-ITP	abasic	25.1 ± 1.5	4.6 ± 1.0	5 460 000
5-CE-ITP	A	0.051 ± 0.002	11 ± 1	4810
5-CE-ITP	C	0.24 ± 0.02	12 ± 1	20 000
5-CE-ITP	G	0.029 ± 0.003	25 ± 7	1160
5-CE-ITP	T	0.076 ± 0.005	63 ± 12	1120
5-CH−ITP	abasic	0.46 ± 0.03	6.2 ± 1.3	74 200
5-CH−ITP	A	0.095 ± 0.003	13 ± 2	7360
5-CH−ITP	C	0.077 ± 0.007	31 ± 9	2480
5-CH−ITP	G	0.011 ± 0.001	23 ± 4	470
5-CH−ITP	T	0.018 ± 0.005	25 ± 10	720

measured for **4** versus **5** corresponds to a $\Delta\Delta G$ of 2.32 kcal/mol. This value most likely reflects the energetic contributions of π-electron density toward facilitating the conformational change step. It is unlikely that desolvation accounts for this energetic difference since the calculated log *P* values for the nucleobase portion of **4** and **5** are essentially identical at 3.15 and 3.63, respectively. Although size constraints may influence the dynamics of the conformational change step (vide infra), it is unlikely that size alone dictates this rate constant, since the surface area for the nucleobase portion of **4** and **5** are nearly identical at 236.4 Å^2 and 240.9 Å^2, respectively.

Although the k_{pol} values vary significantly for nucleotides **4** and **5**, their respective K_D values for incorporation opposite the abasic site are essentially identical (compare 4.6 versus 6.2 μM, respectively). This result is surprising since it was predicted that the K_D for nucleotide **5** would be significantly higher since it lacks significant π-electron density. The identity in binding affinity suggests that efficient dNTP binding can occur even in the absence of π-electron density. Thus, while the rate of the conformational change during translesion DNA synthesis depends on π-electron density, the enhancement in ground-state binding appears related to the size and shape of the non-natural nucleotide.

To further evaluate this mechanism, kinetic rate, and dissociation constants for the insertion of nucleotides **4** and **5** were measured opposite each of the four natural templating nucleobases. As summarized in Table 1, the catalytic efficiency (k_{pol}/K_D) for both compounds is ~300−5,000-fold lower than that for insertion opposite the abasic site. The lower catalytic efficiency is caused by a large reduction in k_{pol} values rather than a perturbation in K_D values. The reduced k_{pol} values are caused by a decrease in the rate of the conformational change step that likely results from the inability of these large, bulky nucleotides to pair with the templating nucleobase. It is also noteworthy that the K_D values for nucleotides **4** and **5** are in the low μM range and relatively independent of templating position. This kinetic phenomenon was previously observed with other 5-substituted indolyl deoxyriboside triphosphates such as **2** and **3** that contain π-electron density.[9,10] The lack of specificity coupled with low K_D values was proposed to reflect the presence of a "non-specific" dNTP binding site that utilized π-electron interactions of the incoming dNTP with aromatic amino acids of the DNA polymerase.[9] The data obtained with nucleotide **4** are consistent with this model. However, the low K_D value measured for nucleotide **5** argues that physical parameters independent of π-electron density such as desolvation and/or size can influence dNTP binding.

These data are used to redefine our original model for translesion DNA synthesis outlined in Figure 4 that accounts for the role of π-electron interactions as well as other biophysical

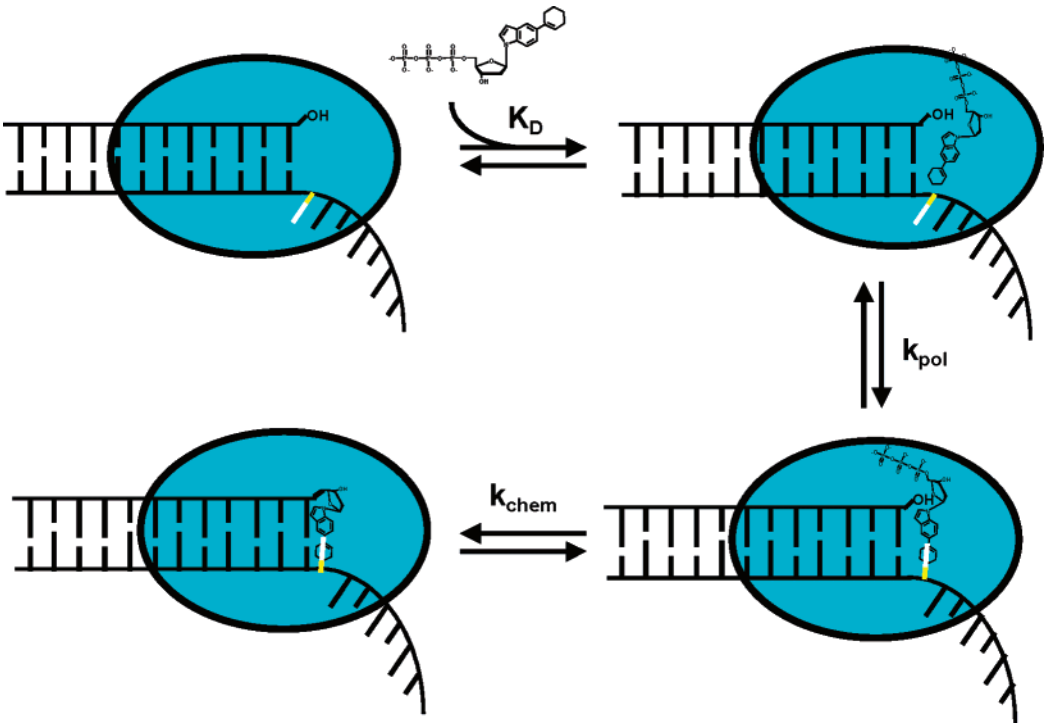

Figure 4. Proposed model for the enzymatic insertion of non-natural nucleotide insertion opposite DNA. The first step represents the binding of dNTP to the polymerase/DNA complex (K_D). The second step represents the conformational change preceding phosphoryl transfer (k_{pol}) required to place the triphosphate moiety in close proximity with the positively charged amino acids as well as to stack the nucleobase portion of the incoming dNTP into the hydrophobic environment of the interior of the duplex DNA. The final step represents the phosphoryl transfer step required for elongation of the primer strand (k_{chem}).

constraints such as size and desolvation. An essential caveat of this revised model is that the templating nucleobase is oriented in a conformation that prevents direct hydrogen-bonding contacts between the templating base and the incoming nucleotide during the initial binding event. This supposition is supported by the structures of several DNA polymerases bound with nucleic acid in the absence and presence of an incoming dNTP.[15] Indeed, these structures provide physical evidence that direct Watson−Crick pairing interactions are precluded due to the expected orientation of the template. In our model, the orientation of the templating nucleobase in an extrahelical position creates a transient "void" in the DNA that provides a functional mimic of an abasic site (Figure 4, step A). It is easy to envision that large, bulky nucleotides such as compounds **4** and **5** can easily fill the "void" produced by the transiently formed abasic site intermediate. Since both molecules are similar in shape and size, their K_D values are essentially identical and independent of the templating nucleobase. In fact, the low binding constant measured for insertion opposite a truly functional abasic site is also consistent with this mechanism. Unlike binding affinity, however, the k_{pol} value is highly dependent upon the presence of a templating nucleobase. We argue that the k_{pol} step (Figure 4, step B) represents the conformational change step required to place the templating base in an interhelical conformation that then allows for proper alignment of the primer-template required for the phosphoryl transfer step (k_{chem}) (Figure 4, step C). When a templating base is present, the rate of this conformational change step is slowed since the shear bulk of the non-natural nucleotide hinders the facile repositioning of the templating nucleobase from an extra- into an intrahelical conformation. At an abasic site, however, the rate of this conformational change is significantly increased since the lack of a templating nucleobase circumvents the need for this repositioning. In fact, large non-natural nucleotides such as **4** and **5** should both be effectively inserted opposite the abasic site since both would provide size and shape complementarity to adequately fill the void. However, the model invoking steric fit is inadequate since, despite having similarities in shape and size, nucleotide **4** has a k_{pol} value that is 55-fold faster than that for nucleotide **5**. The most discernible difference between compounds **4** and **5** is with respect to π-electron density. Thus, while dNTP binding opposite the DNA lesion appears to be driven by shape/size constraints, the rate of the conformational change is linked with the presence of π-electron density at the 5 position of the modified indole.

(15) (a) Franklin, M. C.; Wang, J.; Steitz, T. A. *Cell* **2001**, *105*, 657−667. (b) Hogg, M.; Wallace, S. S.; Doublie, S. *EMBO J.* **2004**, *23*, 1483−1493. Johnson, S. J.; Taylor, J. S.; Beese, L. S. *Proc. Natl. Acad. Sci. U.S.A.* **2003**, *100*, 3895−3900. Li, Y.; Korolev, S.; Waksman, G. *EMBO J.* **1998**, *24*, 7514−7525.

Acknowledgment. The research was supported in part by funds from the NIH (CA118408) to A.J.B. and the Presidential Research Award to I.L.

Supporting Information Available: Detailed characterization of isomeric nucleotide triphosphate. This material is available free of charge via the Internet at http://pubs.acs.org.

JA0546830